Reworking the *Tao–Mo* exchange-correlation functional. I. Reconsideration and simplification ⊘

H. Francisco (ID) ; A. C. Cancio (ID) ; S. B. Trickey ✉ (ID)

Check for updates

View Online   Export Citation   CrossMark

Reworking the *Tao–Mo* exchange-correlation functional. I. Reconsideration and simplification

View Online   Export Citation   CrossMark

H. Francisco,[1,a] (iD) A. C. Cancio,[2] (iD) and S. B. Trickey[3,b] (iD)

AFFILIATIONS

[1] Quantum Theory Project, Department of Physics, University of Florida, Gainesville, Florida 32611, USA

[2] Center for Computational Nanoscience, Department of Physics and Astronomy, Ball State University, Muncie, Indiana 47306, USA

[3] Quantum Theory Project, Department of Physics and Department of Chemistry, University of Florida, Gainesville, Florida 32611, USA

Note: This paper is part of the JCP Festschrift for John Perdew.
a) francisco.hector@ufl.edu
b) Author to whom correspondence should be addressed: trickey@ufl.edu

ABSTRACT

The revised, regularized Tao–Mo (*rreg*TM) exchange-correlation density functional approximation (DFA) [A. Patra, S. Jana, and P. Samal, J. Chem. Phys. **153**, 184112 (2020) and Jana *et al.*, J. Chem. Phys. **155**, 024103 (2021)] resolves the order-of-limits problem in the original TM formulation while preserving its valuable essential behaviors. Those include performance on standard thermochemistry and solid data sets that is competitive with that of the most widely explored meta-generalized-gradient-approximation DFAs (SCAN and r^{2}SCAN) while also providing superior performance on elemental solid magnetization. Puzzlingly however, *rreg*TM proved to be intractable for de-orbitalization via the approach of Mejía-Rodríguez and Trickey [Phys. Rev. A **96**, 052512 (2017)]. We report investigation that leads to diagnosis of how the regularization in *rreg*TM of the z indicator functions (z = the ratio of the von-Weizsäcker and Kohn–Sham kinetic energy densities) leads to non-physical behavior. We propose a simpler regularization that eliminates those oddities and that can be calibrated to reproduce the good error patterns of *rreg*TM. We denote this version as simplified, regularized Tao–Mo, *sreg*TM. We also show that it is unnecessary to use *rreg*TM correlation with *sreg*TM exchange: Perdew–Burke–Ernzerhof correlation is sufficient. The subsequent paper shows how *sreg*TM enables some progress on de-orbitalization.

Published under an exclusive license by AIP Publishing. https://doi.org/10.1063/5.0167868

I. SETTING AND MOTIVATION

The Tao–Mo family[1–4] of meta-generalized-gradient-approximation (meta-GGA) exchange-correlation (XC) density functional approximations (DFAs) has attracted interest for some time. That interest is motivated by the TM DFAs being competitive with the most thoroughly examined meta-GGAs, SCAN[5,6] and r^{2}SCAN[7] when tested against widely used thermochemical data sets (G3X/99 for heats of formation,[8,9] T96-R[10,11] for bond lengths, and T82-F[10,11] for harmonic vibrational frequencies) and also against condensed phase data sets (static-crystal lattice constants and cohesive energies for 55 solids,[12] bulk moduli for 44 solids,[13] and band gaps of 21 insulators and semiconductors[14]). Advantageously, the TM functionals do not have the problem of over-magnetization

of elemental solids exhibited by SCAN and r^{2}SCAN. See Ref. 15 and references therein regarding that problem. As a reminder, note that as is the case with essentially all DFAs, there are test sets on which the advantage is reversed and r^{2}SCAN performance is better than the TM functionals. For two recent examples see Refs. 16 and 17.

Given such interestingly broad applicability for the TM functionals, it was obvious from our pursuit of de-orbitalization[18–20] that the most-refined of the TM family, *rreg*TM, was a worthwhile target. To our surprise and frustration, that de-orbitalization strategy did not work. No simple version or refinement of the procedures in Refs. 18–20 succeeded in reproducing the mean-absolute-deviation error patterns of *rreg*TM on the standard molecular and solid-state data sets just mentioned. We discuss that issue in Paper II.[21] What is

pertinent here is that the de-orbitalization failure suggested the existence of something peculiar or unusual in the $rreg$TM DFA itself. In this paper, we diagnose a source of the problem as being unphysical behavior introduced by regularization of one of the chemical indicator functions used in $rreg$TM. We propose, as a remedy, a simpler regularization and demonstrate, by comparison of performance with the aforementioned test sets, that the simpler version, denoted $sreg$TM, performs as well as the $rreg$TM. In Paper II[21] we show that $sreg$TM enables some progress on de-orbitalization.

In what follows, Sec. II provides the rather intricate formulae for the three versions of TM with highlights of the differences introduced by regularization and revision. Then, in Sec. III we focus on the behavior of the two local chemical behavior indicator functions α and z (definitions below) and the problematic changes in z induced by its regularization in regTM and its use in $rreg$TM. Then a simplified regularization without those problems is presented. Section IV discusses numerical implementation and results on the various test sets. In Sec. V we discuss the effects of the simplified regularization upon consistency with exact constraints, specifically the homogeneous electron gas limit. Section VI provides brief additional observations.

II. TAO–MO VERSIONS

To provide a reasonably self-contained presentation and set notation, we display the complicated equations that define the various TM versions.

As usual in a meta-GGA, the exchange energy (in Hartree atomic units) is written as an enhancement F_x factor relative to the simple local density approximation (LDA)

$$E_x[n] = c_x \int d\mathbf{r} n^{4/3}(\mathbf{r}) F_x(s[n(\mathbf{r})], \tau_s(\mathbf{r})) \quad (1)$$

$$c_x := -\frac{3}{4}\left(\frac{3}{\pi}\right)^{1/3} \quad (2)$$

with the positive definite Kohn–Sham kinetic density[22]

$$\tau_s = \frac{1}{2}\sum_i f_i |\nabla \varphi_i(\mathbf{r})|^2 \quad (3)$$

defined in terms of the Kohn–Sham occupations and orbitals. Two frequently used dimensionless functional variables are

$$s := \frac{|\nabla n(\mathbf{r})|}{2(3\pi^2)^{1/3} n^{4/3}(\mathbf{r})} \quad (4)$$

$$p := s^2 \quad (5)$$

All of the Tao–Mo variants[1–4] have the exchange enhancement factor form

$$F_x^{TM}(p, z, \alpha) = w F_x^{DME} + (1 - w) F_x^{sc}. \quad (6)$$

The various ingredients in it are

$$F_x^{DME}(p, \alpha) = \frac{1}{f^2} + \frac{7R}{9f^4}, \quad (7)$$

with

$$f = [1 + 10(70y/27) + \beta y^2]^{1/10}, \quad (8)$$

and

$$R = 1 + 595(2\lambda - 1)^2 \frac{p}{54} - [z_3 - 3(\lambda^2 - \lambda + 1/2)(z_3 - 1 - z_2/9)]. \quad (9)$$

In turn, the constants are $\beta = 79.873$, $\lambda = 0.6866$ and the auxiliary functions are

$$y := (2\lambda - 1)^2 p \quad (10)$$

$$z_2 := 5p/3 \quad (11)$$

$$z_3 := z_2 + \alpha. \quad (12)$$

The two functions that detect and indicate chemically different regimes, hence enable switching between ingredient functional forms, are defined as

$$\alpha := \frac{\tau_s - \tau_W}{\tau_{TF}} \quad (13)$$

and

$$z := \frac{\tau_W}{\tau_s} = \frac{1}{1 + \frac{3\alpha}{5p}}. \quad (14)$$

The limiting kinetic energy densities involved are Thomas–Fermi

$$\tau_{TF} := c_{TF} n^{5/3}(\mathbf{r}); \quad c_{TF} := \frac{3}{10}(3\pi^2)^{\frac{2}{3}} \quad (15)$$

and von Weizsäcker

$$\tau_W := \frac{1}{8}\frac{|\nabla n(\mathbf{r})|^2}{n(\mathbf{r})}. \quad (16)$$

The other TM X ingredient functional is

$$F_x^{sc}(p, \alpha) := \left\{1 + 10\left[\left(\frac{10}{81} + \frac{50}{729}p\right)p + \frac{146}{2025}\tilde{q}^2 - \frac{73}{405}\tilde{q}\frac{3z}{5}(1 - z)\right]\right\}^{1/10} \quad (17)$$

with the auxiliary quantity

$$\tilde{q}(\alpha, p) := \frac{9}{20}(\alpha - 1) + \frac{2}{3}p. \quad (18)$$

Finally, the function that switches between F_x^{sc} and F_x^{DME} is

$$w(z) := \frac{z^2 + 3z^3}{(1 + z^3)^2}. \quad (19)$$

The original TM X functional has an order-of-limits problem.[23] It is straightforward to rewrite the X enhancement factor, Eq. (6) as a

01 December 2023 14:44:56

function of the variables p and α, Eqs. (5) and (13) respectively. Then the order-of-limits problem is

$$\lim_{p \to 0} \left[\lim_{\alpha \to 0} F_x^{TM}(p, \alpha) \right] \neq \lim_{\alpha \to 0} \left[\lim_{p \to 0} F_x^{TM}(p, \alpha) \right]. \qquad (20)$$

The regularized version of TM[3] regTM removed that anomaly. In it, the X functional itself has essentially the same analytical form as in original TM, as does the w function given in Eq. (19). The X enhancement factor of regTM is given by

$$F_x^{regTM}(p, z, z', \alpha) = w' F_x^{DME} + (1 - w') F_x^{sc}, \qquad (21)$$

and the w function is relabeled as w'. The difference is simply that the original w is evaluated with the variable z' so what is denoted in the original paper as $w'(z')$ is simply $w(z')$.

The important change is the variable z'. It is a regularized version of z given by

$$z'(\alpha, p) = \frac{1}{1 + \frac{3}{5} \left[\frac{\alpha}{p + f_1(\alpha, p)} \right]}, \qquad (22)$$

with the regularizer

$$f_1(\alpha, p) = \frac{(1 - \alpha)^3}{(1 + (d\alpha)^2)^{3/2}} e^{-cp}. \qquad (23)$$

The original z, Eq. (14), is recovered by $f_1 \to 0$. In $f_1(\alpha, p)$ the constants are $c = 3.0$, $d = 1.475$. Note a subtlety. In $F_x^{regTM}(p, z, z', \alpha)$, Eq. (21), z' used *solely* in w', not in F_x^{DME} nor F_x^{sc}.

For clarity about the TM literature, note that in chronological sequence there was a modification of the original TM X functional called revised Tao–Mo, revTM.[2] It is not relevant here. Similarly, the original TM correlation energy functional, which is based on the TPSS and PKZB functionals,[24,25] is not relevant to this work.

The relevant C functional is that proposed for use with regTM, called regTPSS. In essence it is the Perdew–Burke–Ernzerhof (PBE) C functional[26] but with the constant coefficient of the gradient term replaced by a density-dependent coefficient. Again, details are unneeded here; see discussion in Ref. 27. What is relevant for present purposes is the combination of the regTM X functional with the C functional in $rreg$TM.[4] The relevant equations are given in Sec. I of the supplementary material.

III. REGULARIZATION RECONSIDERED

The most refined version of TM is $rreg$TM, so we focus exclusively on it. In our multiple attempts to de-orbitalize it, we found that a major barrier to use of the strategy in Refs. 18 and 19 was the z' indicator. It has some peculiar properties to which we turn.

The original definition of z is Eq. (14)

$$0 \leq z := \frac{\tau_W}{\tau_s} \leq 1 \qquad (24)$$

with τ_W the canonical von Weizsäcker KE density, Eq. (16), and τ_s the Kohn–Sham KE density (in positive semi-definite form). Thus, as shown, z is positive semi-definite. That remains the case when rewritten in terms of α as in the second equality of Eq. (14).
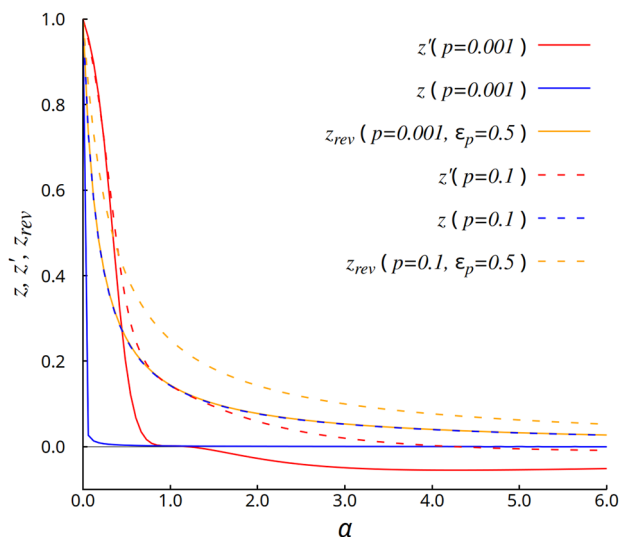

FIG. 1. Comparison of z, z', and z_{rev} for various p values as function of α.

As already mentioned, that expression in terms of α exposes the order-of-limits issue.

Though introduction of the regularization, Eqs. (22) and (23), does remove the order-of-limits problem, it also causes z' to lose the positivity property of z. This follows because $f_1(\alpha) < 0$ for $\alpha > 1$. Figure 1 shows the consequences, namely $z' \leq 0$ for $\alpha \geq 1$ and $p \leq 0.1$. (Ignore, for the moment, the z_{rev} curves.) Regularization with Eq. (23) thus gives z' that breaks the physical meaning of z as a ratio of kinetic energy densities, hence also introduces the possibility of unphysical chemical region detection.

A situation in which $p \approx 0$, $\alpha \approx 1$ is a density that locally at least is close to that of a homogeneous electron gas. Examples include the mid-points of homonuclear diatomic bonds. A bit more detailed insight comes from considering α slightly greater than unity, $\alpha = 1 + \delta$, $0 < \delta \ll 1$ and $p = 0$. For that case, we have

$$f_1(1 + \delta, p = 0) = \frac{(-\delta)^3}{[1 + d^2(1 + \delta)^2]^{3/2}} \qquad (25)$$

$$z'(1 + \delta, 0) = \frac{1}{1 - \frac{3}{5\delta^3} [(1 + \delta)(1 + d^2)^{3/2}]}, \qquad (26)$$

which exhibits the negative behavior. (Though there appears to be the possibility of a negative singularity in z' for small δ, numerical evidence suggests that does not occur.)

It seems impossible to know *a priori* whether the deviation of z' from the positivity of z is consequential for the practical use of $rreg$-TM. In the face of that uncertainty, we deem it prudent not to rely upon an indicator function that violates a constraint that was assumed as an ingredient in constructing TM. The negative z' arises from the factor $(1 - \alpha)^3$ in the numerator of $f_1(\alpha, p)$, Eq. (23). That obviously could be eliminated by changing the numerator to $(1 - \alpha)^2$. The resulting modified z'_{mod} is shown in Fig. 2. While the negative region is removed, the modification still spoils the interpretation of z'_{mod} as a chemical region indicator via the ratio
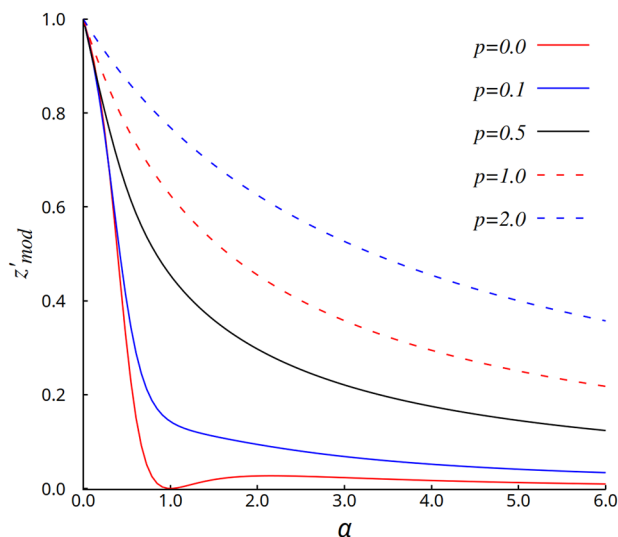
FIG. 2. Modified z' (changed to quadratic numerator in f_1) shown for various p values as function of α.

FIG. 3. z_{rev} function using different values of ϵ_p and p.

of two KE densities, since at fixed small p, z'_{mod} is not monotonic-decreasing with α. Because $p \approx 0$ is the context of any bond, it is quite desirable to have a one-to-one map of α to any approximate z that is a candidate chemical region indicator.

In Ref. 3, the authors remarked on the design choice inherent in regularization: "Note that any small positive definite quantity or real number (greater than zero) can remove the order of limit problem. . . ." Here we take advantage of that design flexibility by observing that a comparatively featureless regularizer avoids the introduction of a modified z that is not positive definite. The function z_{rev} we propose thus is

$$z_{rev}(\alpha, p) = \frac{5p + \epsilon_p}{5p + 3\alpha + \epsilon_p}. \tag{27}$$

We take $0 < \epsilon_p < 1$ with its precise value to be determined by best match on standard test sets to $rreg$ TM results. We denote the X functional obtained from $rreg$TM by replacing z' with z_{rev} as the simplified, regularized TM, $sreg$TM.

It is straightforward to verify that z_{rev} causes no order-of-limits problem of regardless of the value of ϵ_p:

$$\lim_{p \to 0} \left[\lim_{\alpha \to 0} \left[F_x^{sregTM}(p, \alpha) \right] \right] = 1.1132 \tag{28}$$

$$\lim_{\alpha \to 0} \left[\lim_{p \to 0} \left[F_x^{sregTM}(p, \alpha) \right] \right] = 1.1132 \tag{29}$$

The rather featureless behavior of z_{rev} for various choices of ϵ_p and values of p is shown in Fig. 3.

In addition to determining ϵ_p, another design choice remains. One option is to use z_{rev} only to evaluate $w(z)$, i.e., $w(z) \to w(z_{rev})$. We denoted that as $v1$-$sreg$TM. That prescription parallels the use of both z' and z in regTM. The other option is to use z_{rev} to evaluate both the w and the F_x^{sc} function. We denoted that variant as $v2$-$sreg$TM. Since the second variant is simpler and slightly better
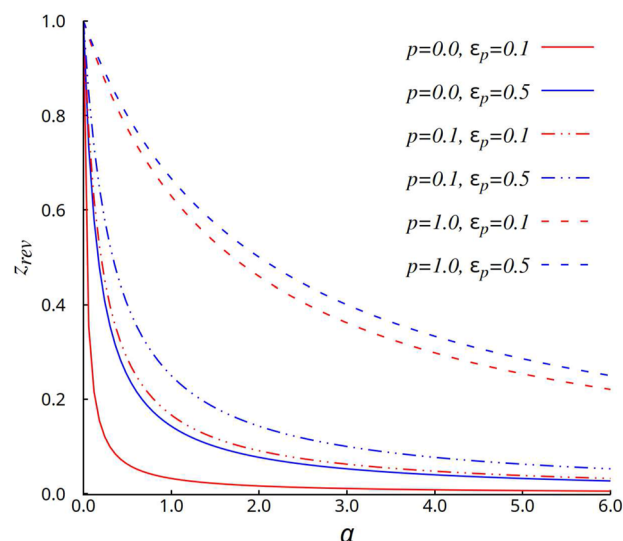
in overall performance, we focus on it. For thoroughness, counterpart results for performance of $v1$-$sreg$TM are in Sec. III of the supplementary material.

In the work with TM and $rreg$TM that stimulated this investigation, we had not experienced any significant anomalies with the $rreg$TM C functional. Therefore, to explore the effects of the fewest changes, as one option we retained $rreg$TM correlation. Along the way, we had learned that original PBE correlation (with the parameter β fixed as in Ref. 26) also works quite well in combination with $rreg$TM exchange. That motivated examination of the combination of $sreg$TM X variants with original PBE C.

IV. IMPLEMENTATION AND NUMERICAL RESULTS

A. Implementation

The two $sreg$TM X functional variants were coded in NWChem-7.0.2[28] to test the molecular test sets and in Vienna *Ab initio* Simulation Package (VASP)-5.4.4[29] for the solid test sets. In NWChem-7.0.2, the calculations were done using a Def2-TZVPP basis set[30] and `xfine` grid settings. Molecular heats of formation were computed according to the procedure established by Curtiss *et al.*[8,9] for the 223 molecules of the G3X/99 test set. The T96-R test set[10,11] was used to study the optimized bond lengths and the T82-F test set[10,11] for the harmonic vibrational frequencies.

For VASP-5.4.4, the computations used PAW (projector augmented wave) pseudopotentials that correspond to the PBE DFA. The default energy cutoff was overridden and set to 800 eV. The precision parameter in VASP was set to `accurate` (PREC=A) and the minimization algorithm used the conjugate gradient method (ALGO=A). Also, approximate thermal smearing of Gaussian type was used with a width of 0.01 eV. Non-spherical contributions within the PAW spheres were included self-consistently (LASPH=.TRUE.). Brillouin zone integrations were performed on a (17 × 17 × 17) Γ-centered, symmetry-reduced Monkhorst–Pack

k-mesh using the tetrahedron method with Blöchl corrections. The ideal c/a ratio was used for hexagonal close-packed structures.

The crystalline symmetries used were the same as in Table II in Ref. 19. The equilibrium lattice constants a_0 and bulk moduli B_0 at $T = 0$ K were determined by calculating the total energy per unit cell in the range of $V_0 \pm 10\%$, where V_0 is the equilibrium unit cell volume. A 12-point series of values was fitted to the stabilized jellium equation of state (SJEOS).[31] Static-crystal lattice constants and cohesive energies were calculated for 55 solids[12] and bulk moduli for 44 solids,[13] as were Kohn–Sham band gaps of 21 insulators and semiconductors.[14] All the values were compared with the experimental values. For cohesive energy determination, the isolated atom energies were approximated by use of a $14 \times 15 \times 16$ Å^3 unit cell and Gamma-point Brillouin zone sampling.

Regarding computational technique, it is important to mention that the derivative of the original function z, Eq. (14) with respect to the α and p variables can exhibit some numerical problems when those variables go to zero simultaneously. To a lesser extent, that also is true with z_{rev}. To address those numerical problems, the condition was imposed that if both those derivatives are less than 1×10^{-10} at a grid point, then both derivatives are set to zero there.

B. Computed results—Test sets

The initial computational task was to determine the most appropriate value for ϵ_p in the z_{rev} function. Since our objective was to reproduce the real-system results from $rreg$TM as closely as possible, we did calculations on the molecular test sets with a range of ϵ_p values for each variant: $\epsilon_p = 0.01, 0.1, 0.2, 0.3, 0.4, 0.5, 0.6$. In Fig. 3, one can see the behavior of the z_{rev} function for different values of ϵ_p and p, while Fig. 1 displays a comparison between the z_{rev} function and the z' and z functions.

For the $v2$-$sreg$TM X functional in combination with the $rreg$TM C functional, Table I shows that as ϵ_p grows, the errors on the three test sets decrease, until the error on the G3X/99 set increases again at $\epsilon_p = 0.6$. Because the object is to match the behavior of $rreg$TM on the test sets, we selected among those values following the strategy used earlier in de-orbitalization.[18] Thus we picked the ϵ_p value that gave MAD (mean absolute deviation) results on the three molecular test sets closest to those from $rreg$TM, based upon semi-quantitative comparison by inspection. Because heats of formation are variational and because bond length and frequency MADs tend to be comparatively insensitive, we prioritized heat of formation MAD. With $\epsilon_p = 0.5$, the MAD error pattern on the molecular test sets is essentially indistinguishable from the error pattern for the $rreg$TM XC functional. (Note that the individual molecule results are tabulated in the supplementary material). Then we confirmed that choice from behavior on the solid test sets. Well after we had chosen $\epsilon_p = 0.5$ for detailed further study, we found (from fitting the results in Table I) that the minimum heat of formation MAD actually is at $\epsilon_p = 0.452$. However,

TABLE I. Molecular test set results for the $v2$-$sreg$TM exchange functional combined with the $rreg$TM correlation functional for different values of ϵ_p. Heat of formation errors in kcal mol^{-1}, bond length errors in Å, and frequency errors in cm^{-1}.

		$v2$-$sreg$TM X + $rreg$TM C							
	ϵ_p	0.01	0.1	0.2	0.3	0.4	0.5	0.6	$rreg$TM XC
Heats	ME	3.200	1.769	0.275	−1.103	−2.364	−3.512	−4.554	−3.790
of formation	MAD	8.689	7.633	6.779	6.211	5.903	5.895	6.183	5.612
Bonds	ME	0.015	0.015	0.014	0.014	0.013	0.013	0.011	0.012
	MAD	0.018	0.017	0.017	0.016	0.016	0.015	0.014	0.014
Frequencies	ME	−25.934	−24.61	−23.225	−21.847	−20.524	−19.275	−18.165	−21.011
	MAD	36.647	35.986	35.429	35.000	34.562	34.272	34.054	35.578

TABLE II. Summary of molecular test set results for the $v2$-$sreg$TM exchange functional (with $\epsilon_p = 0.5$) combined with the $rreg$TM correlation functional and also with PBE C, vs $rreg$TM X combined with PBE C, all compared with PBE XC and r^{2}SCAN XC. Heat of formation errors in kcal mol^{-1}, bond length errors in Å, and frequency errors in cm^{-1}.

	X	$rreg$TM	$v2$-$sreg$TM	$rreg$TM	$v2$-$sreg$TM	r^{2}SCAN	PBE
	C	$rreg$TM	$rreg$TM	PBE	PBE	r^{2}SCAN	PBE
Heats of formation	ME	−3.79	−3.512	−2.208	−1.520	−3.145	−20.878
	MAD	5.612	5.895	5.452	5.354	4.488	21.385
Bonds	ME	0.012	0.013	0.008	0.008	0.005	0.018
	MAD	0.014	0.015	0.011	0.011	0.010	0.018
Frequencies	ME	−21.011	−19.275	−4.667	−2.865	11.336	−33.781
	MAD	35.578	34.272	25.183	24.138	30.899	43.613

TABLE III. Comparison of solid system errors for DFA combinations as in Table II for four solid test sets. Equilibrium lattice constant errors in Å, cohesive energy errors in eV/atom, bulk modulus errors in GPa, and Kohn–Sham band gap errors in eV.

| | | X $rreg$TM | $v2$-$sreg$TM | $rreg$TM | $v2$-$sreg$TM | r^{2}SCAN | PBE |
		C $rreg$TM	$rreg$TM	PBE	PBE	r^{2}SCAN	PBE
Lattice constants	ME	0.000	0.004	−0.006	−0.002	0.026	0.046
	MAD	0.029	0.031	0.028	0.029	0.037	0.053
Cohesive energies	ME	0.212	0.159	0.248	0.199	−0.134	−0.070
	MAD	0.251	0.216	0.288	0.251	0.238	0.252
Bulk moduli	ME	1.856	0.223	4.375	2.732	1.367	−9.704
	MAD	6.740	6.602	7.200	6.542	5.963	11.022
Band gaps	ME	−1.52	−1.53	−1.42	−1.44	−1.20	−1.69
	MAD	1.52	1.53	1.42	1.44	1.20	1.69

preservation of the second-order gradient expansion (see Sec. V) is at $\epsilon_p = 0.586\,58$, so 0.5 ends up being an unexpectedly useful compromise value.

In Table II we show the effect of combining $sreg$TM with $rreg$TM correlation and, alternatively, with ordinary PBE correlation (fixed β value). One can see that on all three molecular tests, $v2$-$sreg$TM X with either $rreg$TM C or PBE C, is as good or better than the original $rreg$TM X with the corresponding C functional. Either combination is almost as good as r^{2}SCAN on heat of formation, as good on bond lengths, and better on harmonic frequencies.

Given the fidelity of $v2$-$sreg$TM X to $rreg$TM X for the error pattern on the three molecular test sets, we turn to the solid test sets. Table III shows that the behavior of $v2$-$sreg$TM variant is consistent with that for molecular test sets. For the solids, $v2$-$sreg$ TM X in combination with $rreg$TM C behaves very much like the $rreg$TM XC functional. For both lattice constants and cohesive energies, $v2$-$sreg$TM X plus $rreg$TM C is better than r^{2}SCAN and a bit worse on bulk moduli and Kohn-Sham band gaps. The combination $v2$-$sreg$TM X with PBE C is as good (but no better) on cohesive energies than $rreg$TM XC but better than $rreg$TM X + PBE C. Otherwise $v2$-$sreg$TM X with PBE C is essentially indistinguishable from $v2$-$sreg$TM X plus $rreg$TM C. Use of $v1$-$sreg$TM X instead of $v2$-$sreg$TM X degrades bulk modulus performance for solids, but otherwise is comparable with the second variant. Since, however, the

second variant is simpler and slightly better in overall performance, we prefer it. (Again, all of the individual solid results are tabulated in the supplementary material).

C. Computed results—Elemental magnetization

The reported experimental magnetic moments of elemental bcc Fe, fcc Co, and fcc Ni are 2.22, 1.72, and, 0.62 μ_B respectively.[32,33] It has been known for a long time that these values are not easy to match at calculated equilibrium lattice parameters with a simple DFA. LDA was a failure. More recently it was found that the SCAN DFA over-magnetizes some elemental transition metals.[34–39] A summary discussion and diagnosis of the cause is in Ref. 15. It also is known that $rreg$TM does not have this problem.[4] As we remarked at the outset, that distinction was one of the original motivations for our investigation.

Thus, we calculated the saturation magnetization of bcc Fe, fcc Co, and fcc Ni at the calculated equilibrium lattice constants for each of the relevant XC DFAs. The results (from calculations at 50 fixed moments) are displayed in Table IV. For bcc Fe, the functionals PBE and $v2$-$sreg$TM X + PBE C provide the most realistic saturation magnetization values with a difference of 0.04 μ_B relative to the experimental values. The $v2$-$sreg$TM X + $rreg$TM C, which provided generally good results on the molecular and solid test sets, also provides an essentially indistinguishable result from

TABLE IV. Saturation magnetic moments in μ_B for some 3d solids with $v2$-$sreg$TM X functional (with $\epsilon_p = 0.5$) combined with the $rreg$TM correlation functional, as well as with PBE C vs $rreg$TM X combined with PBE C, all compared with PBE XC and r^{2}SCAN XC. "Exp." denotes the experimental saturation magnetization.

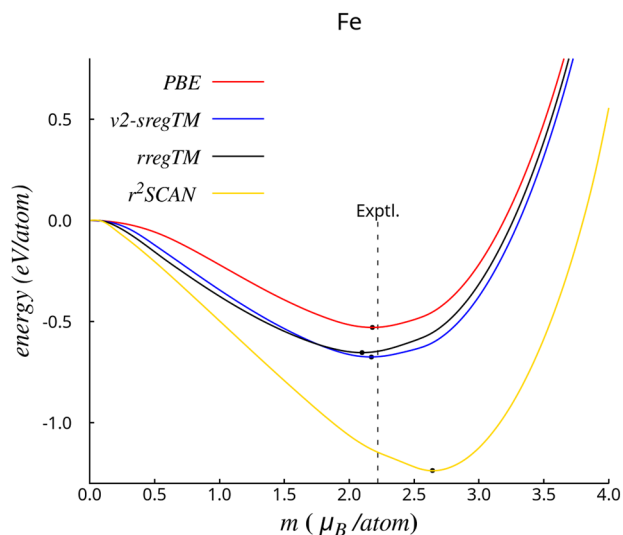|	Exp.	X C	$rreg$TM $rreg$TM	$v2$-$sreg$TM $rreg$TM	$rreg$TM PBE	$v2$-$sreg$TM PBE	r^{2}SCAN r^{2}SCAN	PBE PBE
Fe	2.22		2.10	2.17	2.10	2.18	2.64	2.18
Co	1.72		1.72	1.73	1.72	1.74	1.83	1.64
Ni	0.62		0.68	0.66	0.68	0.66	0.72	0.63

FIG. 4. Fixed spin moment energy for bcc Fe at the calculated equilibrium lattice parameter, on a per-atom basis for PBE XC, $v2$-$sreg$TM X + $rreg$TM C, $rreg$TM XC, and r^{2}SCAN. "Exptl." denotes the experimental saturation magnetization.

FIG. 6. As in Fig. 4 for fcc Ni.

$v2$-$sreg$TM X + PBE C for the bcc Fe magnetization. Consistent with previous findings, the least accurate result is from r^{2}SCAN XC. For fcc Co, magnetization results from the DFAs $rreg$TM XC, and $rreg$TM X + PBE C are indistinguishable from the experimental value. Clearly, the DFAs that use $sreg$TM exchange give essentially indistinguishable results for Co, while r^{2}SCAN XC is the least accurate. For fcc Ni, the results from all the DFAs are grouped tightly, but again with the r^{2}SCAN XC error the largest.

It is not just the saturation magnetization that is different. Figures 4–6 show that the r^{2}SCAN description of the energetic
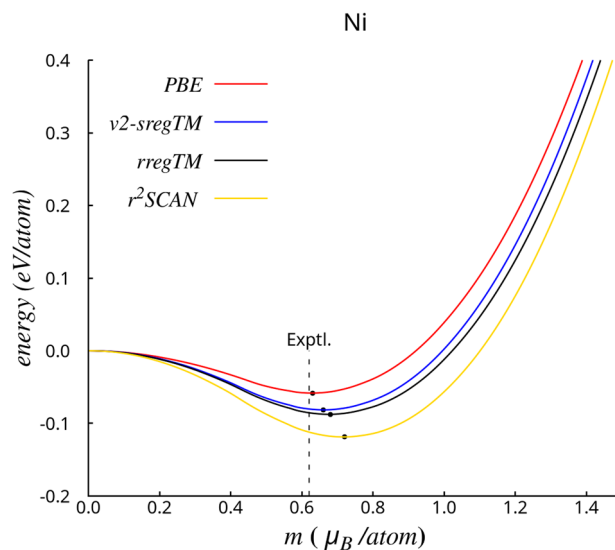

FIG. 5. As in Fig. 4 for fcc Co.

behavior with respect to magnetization is qualitatively different from that provided by the TM DFAs or by PBE. The distinction in depth of energy minima is about a factor of two for bcc Fe and fcc Co, but even for fcc Ni it is about 11.5%. Details are tabulated in the supplementary material. Note also that the r^{2}SCAN energy wells are broader and shaped differently from those of the other DFAs.

V. IMPACT OF SIMPLIFICATION: SLOWLY-VARYING ELECTRON GAS

Replacement of the regularized z', Eq. (22) in $rreg$TM with the much simpler regularized z_{rev}, Eq. (27) is not without a cost. Specifically, the removed regularizer, f_1 Eq. (23), was designed to retain gradient expansion satisfaction. Thus it remains to assess the impact of its removal. The most obvious case of concern is the limit of the slowly varying electron gas, defined by p, $|q| \ll 1$, where $q := \nabla^2 n / 4k_F^2 n$ [$k_F := (3\pi^2 n)^{1/3}$] is the reduced Laplacian of the density. In that regime, the factor $\delta = \alpha - 1$ also $\ll 1$, and has the gradient expansion $20q/9 - 40p/27$. The homogeneous electron gas limit is characterized by $p = q = \delta = 0$.

As noted above, it is in this regime that the strange kink in z' and the transition to negative z' occurs, both caused by the numerator δ^3 of $f_1(\alpha, p)$. This choice guarantees that as p and α tend to zero, the changes made going from z to z', and subsequently w to w' and thus to the X enhancement factor F_x^{TM1} going to F_x^{regTM},[3] are at most third order in the variables p and q, hence sixth order in the gradient expansion of exchange. The $rreg$TM form of z' thus preserves the constraint of returning the exact gradient expansion for exchange through fourth-order that is a feature of the original TM X.

This is no longer the case with z_{rev}. With the value of $\epsilon_p = 0.5$ determined pragmatically (recall above), the homogeneous electron
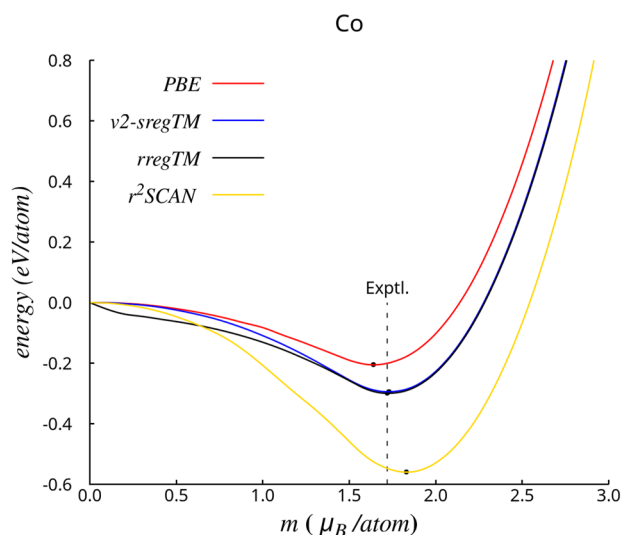
gas limit of $z_{rev}(p = 0, \alpha = 1) = 1/7$ [Eq. (27)] rather than the correct limit of zero. This leads to a value of $w'(0, 1) \equiv w(z_{rev}(0, 1)) = 0.028\,99$, rather than the design limit of 0.

However the impact of these discrepancies is fortunately small. In the homogeneous electron gas limit, $F_x^{DME} = 1$ and $F_x^{sc} = 1$ so that the overall value for the enhancement factor in this limit [Eq. (21)] is trivially unity, regardless of the value of w'. Thus all variants of *sreg*TM return the correct homogeneous electron gas limit.

The next step is compliance with the second-order gradient expansion for the slowly-varying electron gas. For exchange, it is given by

$$F_x \rightarrow F_x^{(2)} = 1 + \frac{10}{81}p, \; p \rightarrow 0. \quad (30)$$

There are two sources of error introduced by the improper value $z_{rev}(p = 0, \alpha = 1) \neq 0$ in the slowly-varying limit. First, as w' does not tend to zero properly, F_x^{DME} makes a spurious contribution to the gradient expansion. This creates an error in the slowly-varying limit for both variants of *sreg*TM we have studied here. But for *v2* only, there is a second error, from the use of z_{rev} in F_x^{SC}. As shown in the supplementary material, the net effect of these two contributions for any given ϵ_p is to produce an error in the second-order gradient expansion, $\delta F_x^{(2)}$, of

$$\delta F_x^{(2)} = \delta_q^{SC} q + w_0 \left[\left(\delta_p^{DME} - \frac{10}{81} \right) p + \left(\delta_q^{DME} - \delta_q^{SC} \right) q \right] \quad (31)$$

where

$$\delta_q^{SC} = -\frac{73}{225} \frac{\epsilon_p}{(3 + \epsilon_p)^2} \quad (32)$$

$$\delta_p^{DME} = 0.327\,39 \quad (33)$$

$$\delta_q^{DME} = -0.251\,55 \quad (34)$$

are coefficients deriving from F_x^{SC} and F_x^{DME} respectively, and further,

$$w_0(\epsilon_p) := w(z_0(\epsilon_p)), \quad (35)$$

$$z_0(\epsilon_p) := z_{rev}(p = 0, \alpha = 1) = \frac{\epsilon_p}{3 + \epsilon_p}. \quad (36)$$

Equation (31) can be simplified further by noting that an enhancement factor linear in the the reduced Laplacian variable q yields the same exchange energy as one linear in $p/3$, via integration by parts.[40] The terms in p and q therefore may be combined to produce a single error function with respect to p alone. As δ_q^{SC} is negative and the second term in this equation is net positive, one thus may search for an ϵ_p value for which the two contributions cancel. A numerical solution yields $\epsilon_p = 0.585\,68$, which is happily close to the value of 0.5 chosen pragmatically. This error cancellation only occurs for *v2-sreg*TM. For *v1-sreg*TM, $\delta_q^{sc} = 0$ and the net error is positive for any value of ϵ_p. This provides another reason, therefore, to prefer *v2-sreg*TM.

Clearly this result also can be used to define a *v3-sreg*TM which is second-order gradient expansion compliant, simply by replacing $\epsilon_p = 0.5$ with the gradient-expansion-compliant value of 0.585\,68. We have tested this variant against the molecular and solid-state test sets already mentioned. Detailed tabulations are in the supplementary material. The gradient-expansion-compliant *v3-sreg*TM gets heat of formation MAD that are about 4% worse than those of *v2-sreg*TM, namely 6.128 kcal/mol vs 5.895. That is not surprising, since *v2-sreg*TM was chosen to optimize this measure, and the optimum ϵ_p value for least heat-of-formation MAD is around 0.45. Recall Sec. IV B. There is almost no difference on the bond distance and frequency MADs. However, *v3-sreg*TM improves over *v2-sreg*TM for solids, which are closer to the GE limit. It is slightly less than 3% better on solid cohesive energy and 2.5% on bulk modulus. So a small violation of second-order gradient expansion in *v2-sreg*TM provides a slightly more balanced overall treatment of molecules and solids than does satisfaction of the second-order gradient expansion in *v3-sreg*TM.

VI. CONCLUDING REMARKS

We have presented an analysis of the *rreg*TM X functional that shows that its regularization introduces peculiar behavior in the z iso-orbital indicator. We have argued that the regularization employed in *reg*TM is unphysical, a fact that justifies exploitation of a simplified regularization. Further, we have shown that the simplified regularization is just as effective on standard molecular and crystalline data sets as the *rreg*TM regularization and that both the *v1-sreg*TM and *v2-sreg*TM exchange with *rreg*TM correlation retains the realistic handling of $3d$ elemental solid magnetism given by *rreg*TM.

We also have demonstrated a further simplification. Namely, PBE correlation is essentially as good a choice for use with our *sreg*TM functionals as is *rreg*TM correlation, with the benefit that the required computational effort is reduced (at least slightly) by such use of a GGA instead of a meta-GGA correlation term. In sum, *sreg*TM appears to embody the full capabilities of the original TM DFA without the drawbacks of subsequent efforts to remove its limitations. The price paid is a small violation of one of the basic constraints of non-empirical DFAs, an illustration of the difficult design choices imposed by the confrontation of rigorous constraints with experimental data.

SUPPLEMENTARY MATERIAL

The supplementary material provides equations for the *rreg*TM correlation functional, details of the analysis of the weakly varying limit and compliance with the gradient expansion of the new regularization, full comparative numerical results for the *v1-sreg*TM version of the new regularization, detailed magnetization results, and system-by-system tabulation of results for each of the molecular and crystalline test sets.

ACKNOWLEDGMENTS

AUTHOR DECLARATIONS

Conflict of Interest

The authors have no conflicts to disclose.

Author Contributions

H. Francisco: Conceptualization (equal); Data curation (lead); Formal analysis (supporting); Investigation (lead); Methodology (lead); Software (lead); Validation (lead); Visualization (equal); Writing – review & editing (supporting). **A. C. Cancio**: Conceptualization (equal); Data curation (equal); Formal analysis (equal); Funding acquisition (supporting); Methodology (equal); Project administration (supporting); Software (equal); Supervision (equal); Validation (equal); Visualization (lead); Writing – original draft (supporting); Writing – review & editing (equal). **S. B. Trickey**: Conceptualization (equal); Data curation (supporting); Formal analysis (equal); Funding acquisition (lead); Investigation (supporting); Methodology (equal); Project administration (lead); Resources (equal); Supervision (lead); Validation (equal); Writing – original draft (lead); Writing – review & editing (equal).

DATA AVAILABILITY

The data that support the findings of this study are available within the article and its supplementary material. Code for NWChem and VASP modications needed to implement *v2-sreg*TM and *v2-sreg*TM-L (discussed in Paper II[21]) is available to experienced users upon request to the authors.

REFERENCES

[1] J. Tao and Y. Mo, Phys. Rev. Lett. **117**, 073001 (2016).

[2] S. Jana, K. Sharma, and P. Samal, J. Phys. Chem. A **123**, 6356 (2019).

[3] A. Patra, S. Jana, and P. Samal, J. Chem. Phys. **153**, 184112 (2020).

[4] S. Jana, S. K. Behera, S. Śmiga, L. A. Constantin, and P. Samal, J. Chem. Phys. **155**, 024103 (2021).

[5] J. Sun, A. Ruzsinszky, and J. P. Perdew, Phys. Rev. Lett. **115**, 036402 (2015).

[6] J. Sun, R. C. Remsing, Y. Zhang, Z. Sun, A. Ruzsinszky, H. Peng, Z. Yang, A. Paul, U. Waghmare, X. Wu, M. L. Klein, and J. P. Perdew, Nat. Chem. **8**, 831 (2016).

[7] J. W. Furness, A. D. Kaplan, J. Ning, J. P. Perdew, and J. Sun, J. Phys. Chem. Lett. **11**, 8208 (2020).

[8] L. A. Curtiss, K. Raghavachari, P. C. Redfern, and J. A. Pople, J. Chem. Phys. **106**, 1063 (1997).

[9] L. A. Curtiss, P. C. Redfern, K. Raghavachari, and J. A. Pople, J. Chem. Phys. **114**, 108 (2001).

[10] V. N. Staroverov, G. E. Scuseria, J. Tao, and J. P. Perdew, J. Chem. Phys. **119**, 12129 (2003).

[11] V. N. Staroverov, G. E. Scuseria, J. Tao, and J. P. Perdew, J. Chem. Phys. **121**, 11507 (2004).

[12] H. Peng, Z.-H. Yang, J. P. Perdew, and J. Sun, Phys. Rev. X **6**, 041005 (2016).

[13] F. Tran, J. Stelzl, and P. Blaha, J. Chem. Phys. **144**, 204120 (2016).

[14] F. Tran and P. Blaha, J. Phys. Chem. A **121**, 3318 (2017).

[15] D. Mejía-Rodríguez and S. B. Trickey, Phys. Rev. B **100**, 041113(R) (2019).

[16] R. Kingsbury, A. S. Gupta, C. J. Bartel, J. M. Munro, S. Dwaraknath, M. Horton, and K. A. Persson, Phys. Rev. Mater. **6**, 013801 (2022).

[17] M. Kothakonda, A. D. Kaplan, E. B. Isaacs, C. J. Bartel, J. W. Furness, J. Ning, C. Wolverton, J. P. Perdew, and J. Sun, ACS Mater. Au **3**, 102–111 (2023).

[18] D. Mejía-Rodríguez and S. B. Trickey, Phys. Rev. A **96**, 052512 (2017).

[19] D. Mejía-Rodríguez and S. B. Trickey, Phys. Rev. B **98**, 115161 (2018).

[20] D. Mejía-Rodríguez and S. B. Trickey, Phys. Rev. B **102**(12), 121109 (2020).

[21] H. Francisco, A. C. Cancio, and S. B. Trickey, "Reworking the Tao–Mo exchange-correlation functional. II. De-orbitalization," J. Chem. Phys. **159**, 214103 (2023).

[22] W. Kohn and L. J. Sham, Phys. Rev. **140**, A1133–A1138 (1965).

[23] J. W. Furness, N. Sengupta, J. Ning, A. Ruzsinszky, and J. Sun, J. Chem. Phys. **152**, 244112 (2020).

[24] J. Tao, J. P. Perdew, V. N. Staroverov, and G. E. Scuseria, Phys. Rev. Lett. **91**, 146401 (2003).

[25] J. P. Perdew, S. Kurth, A. Zupan, and P. Blaha, Phys. Rev. Lett. **82**, 2544 (1999).

[26] J. P. Perdew, K. Burke, and M. Ernzerhof, Phys. Rev. Lett. **77**, 3865 (1996); Erratum **78**, 1396 (1997).

[27] A. Ruzsinszky, J. Sun, B. Xiao, and G. I. Csonka, J. Chem. Theory Comput. **8**, 2078 (2012).

[28] E. Aprà, E. J. Bylaska, W. A. de Jong, N. Govind, K. Kowalski, T. P. Straatsma, M. Valiev, H. J. J. van Dam, Y. Alexeev, J. Anchell, V. Anisimov, F. W. Aquino, R. Atta-Fynn, J. Autschbach, N. P. Bauman, J. C. Becca, D. E. Bernholdt, K. Bhaskaran-Nair, S. Bogatko, P. Borowski, J. Boschen, J. Brabec, A. Bruner, E. Cauët, Y. Chen, G. N. Chuev, C. J. Cramer, J. Daily, M. J. O. Deegan, T. H. Dunning, Jr., M. Dupuis, K. G. Dyall, G. I. Fann, S. A. Fischer, A. Fonari, H. Früchtl, L. Gagliardi, J. Garza, N. Gawande, S. Ghosh, K. Glaesemann, A. W. Götz, J. Hammond, V. Helms, E. D. Hermes, K. Hirao, S. Hirata, M. Jacquelin, L. Jensen, B. G. Johnson, H. Jónsson, R. A. Kendall, M. Klemm, R. Kobayashi, V. Konkov, S. Krishnamoorthy, M. Krishnan, Z. Lin, R. D. Lins, R. J. Littlefield, A. J. Logsdail, K. Lopata, W. Ma, A. V. Marenich, J. Martín del Campo, D. Mejía Rodríguez, J. E. Moore, J. M. Mullin, T. Nakajima, D. R. Nascimento, J. A. Nichols, P. J. Nichols, J. Nieplocha, A. Otero-de-la-Roza, B. Palmer, A. Panyala, T. Pirojsirikul, B. Peng, R. Peverati, J. Pittner, L. Pollack, R. M. Richard, P. Sadayappan, G. C. Schatz, W. A. Shelton, D. W. Silverstein, D. M. A. Smith, T. A. Soares, D. Song, M. Swart, H. L. Taylor, G. S. Thomas, V. Tipparaju, D. G. Truhlar, K. Tsemekhman, T. Van Voorhis, Á. Vázquez-Mayagoitia, P. Verma, O. Villa, A. Vishnu, K. D. Vogiatzis, D. Wang, J. H. Weare, M. J. Williamson, T. L. Windus, K. Wolinski, A. T. Wong, Q. Wu, C. Yang, Q. Yu, M. Zacharias, Z. Zhang, Y. Zhao, and R. J. Harrison, J. Chem. Phys. **152**, 184102 (2020).

[29] G. Kresse and D. Joubert, Phys. Rev. B **59**, 1758 (1999).

[30] F. Weigend and R. Ahlrichs, Phys. Chem. Chem. Phys. **7**, 3297 (2005).

[31] A. B. Alchagirov, J. P. Perdew, J. C. Boettger, R. C. Albers, and C. Fiolhais, Phys. Rev. B **63**, 224115 (2001).

[32] H. Danan, A. Herr, and A. J. P. Meyer, J. Appl. Phys. **39**, 669 (1968).

[33] H. P. Meyers and W. Sucksmith, Proc. R. Soc. London, Ser. A **207**, 427 (1951).

[34] E. B. Isaacs and C. Wolverton, Phys. Rev. Mater. **2**, 063801 (2018).

[35] S. Jana, A. Patra, and P. Samal, J. Chem. Phys. **149**, 044120 (2018).

[36] A. H. Romero and M. J. Verstraete, Eur. Phys. J. B **91**, 193 (2018).

[37] M. Ekholm, D. Gambino, H. J. M. Jönsson, F. Tasnádi, B. Alling, and I. A. Abrikosov, Phys. Rev. B **98**, 094413 (2018).

[38] Y. Fu and D. J. Singh, Phys. Rev. Lett. **121**, 207201 (2018).

[39] Y. Fu and D. J. Singh, Phys. Rev. B **100**, 045126 (2019).

[40] A. C. Cancio, C. E. Wagner, and S. A. Wood, Int. J. Quantum Chem. **112**, 3796 (2012).

01 December 2023 14:44:56